Global Change Biology

WILEY

Global Change Biology

RESEARCH ARTICLE OPEN ACCESS

Harnessing Microbes to Weather Native Silicates in Agricultural Soils for Scalable Carbon Dioxide Removal

Tania Timmermann[1] | Christopher Yip[1] | Yun-Ya Yang[1] | Kimberly A. Wemmer[1] | Anupam Chowdhury[1] | Daniel Dores[1] | Taichi Takayama[1] | Sharon Nademanee[1] | Bjorn A. Traag[1] | Kazem Zamanian[2] | Bernardo González[3] | Daniel O. Breecker[4] | Noah Fierer[5,6] | Eric W. Slessarev[7,8] | Gonzalo A. Fuenzalida-Meriz[1]

[1]Andes Ag, Inc., Alameda, California, USA | [2]Institute of Earth System Sciences, Section Soil Science, Leibniz University of Hannover, Hannover, Germany | [3]Laboratorio de Bioingeniería, Facultad de Ingeniería y Ciencias, Universidad Adolfo Ibáñez, Santiago, Chile | [4]Department of Geological Sciences, University of Texas at Austin, Austin, Texas, USA | [5]Department of Ecology and Evolutionary Biology, University of Colorado Boulder, Boulder, Colorado, USA | [6]Cooperative Institute for Research in Environmental Sciences, University of Colorado Boulder, Boulder, Colorado, USA | [7]Department of Ecology and Evolutionary Biology, Yale University, New Haven, Connecticut, USA | [8]Yale Center for Natural Carbon Capture, Yale University, New Haven, Connecticut, USA

Correspondence: Gonzalo A. Fuenzalida-Meriz (gonzalofuenzalida@gmail.com)

Received: 7 February 2025 | **Revised:** 9 April 2025 | **Accepted:** 12 April 2025

Keywords: agriculture | carbon dioxide removal (CDR) | carbonate precipitation | microbial soil treatment | microbially-mediated silicate weathering | native silicate minerals | soil inorganic carbon (SIC)

ABSTRACT

Anthropogenic carbon emissions contribute significantly to the greenhouse effect, resulting in global warming and climate change. Thus, addressing this critical issue requires innovative and comprehensive solutions. Silicate weathering moderates atmospheric CO_2 levels over geological time, but it occurs too slowly to counteract anthropogenic emissions effectively. Here, we show that the microorganism *Bacillus subtilis* strain MP1 promotes silicate weathering across different experimental setups with various levels of complexity. First, we found that MP1 was able to form a robust biofilm in the presence of feldspar and significantly increased ($p < 0.05$) silicate dissolution rates, pH, and calcium carbonate formation in culture experiments. Second, in mesocosm experiments, we found that MP1 enhanced the silicate weathering rate in soil by more than six times compared to the untreated control. In addition, soil inorganic carbon increased by 20%, and the concentrations of ions, including calcium, magnesium, and iron, were also elevated under the MP1 treatment. More importantly, when applied as a seed treatment on eight soybean fields, we found that MP1 significantly ($p < 0.05$) boosted soil inorganic carbon, leading to a gross accrual of 2.02 tonnes of inorganic carbon per hectare annually. Our findings highlight the potential of enhancing native silicate weathering with microorganisms in agricultural fields to increase soil inorganic carbon, contributing to climate change mitigation.

1 | Introduction

Global warming of 1.5°C above pre-industrial levels would dramatically increase the risk of extreme weather events, more frequent and more intense wildfires, rising sea levels, and changes in flood and drought patterns (Armstrong McKay et al. 2022). There is an urgent need for novel carbon dioxide removal (CDR) approaches to reduce atmospheric CO_2 levels and offset some of the anthropogenic contributions to climate change (Solomon 2007). There are several potential strategies, including those deployed on agricultural soils, which represent about 10% of the global terrestrial land surface area (Potapov et al. 2022). Fierer and Walsh proposed that enhanced microbially mediated weathering and microbially induced carbonate precipitation are two potential strategies to accelerate soil carbon sequestration (Fierer and Walsh 2023).

Silicate weathering plays a crucial role in Earth's long-term carbon cycle by regulating atmospheric CO_2 levels (Walker et al. 1981; Brantley et al. 2023). Silicate weathering releases ions such as calcium (Ca^{2+}) and magnesium (Mg^{2+}), which contribute to soil fertility and the formation of soil inorganic carbon (SIC) (Wilson 2004; Sanderman 2012). Although weathering can deplete soil primary minerals and reduce nutrient availability over time, this process typically occurs over thousands to millions of years (Chadwick et al. 2022). Various lines of evidence suggest that microorganisms may have a crucial but often underestimated role in weathering (Wild et al. 2022). For example, microorganisms such as *Bacillus* can enhance the rate of silicate weathering by establishing close associations with mineral surfaces and environments and by affecting kinetic parameters (e.g., pH and redox potential) (Mo and Lian 2011). One of the key mechanisms driving microbially enhanced weathering is the reduction of pH through the release of low-molecular-weight organic acids and dissolved CO_2 (Vicca et al. 2022; Ahmed and Holmström 2014; Basak and Biswas 2009). Previous studies have demonstrated that *Bacillus mucilaginosus* and *Bacillus edaphicus*, potassium-solubilizing microorganisms, excrete organic acids (e.g., oxalic and citric acids) that dissolve potassium sources from mica or chelate silicon ions, thereby enhancing crop biomass yield (Basak and Biswas 2009; Ahmad et al. 2020). Through this process, microorganisms contribute to soil development, the biogeochemical cycling of essential elements, and maintenance of soil fertility (Banfield et al. 1999; Barker et al. 1997; Homann et al. 2018; Zhao et al. 2023; Ribeiro et al. 2020).

To better understand the enhanced weathering processes facilitated by *Bacillus*, numerous studies have been conducted across various scales, including mesocosms (Amann et al. 2020; Vienne et al. 2022; Niron et al. 2024) and field trials (Beerling et al. 2024). Niron et al. (2024) investigated the effect of *Bacillus subtilis* on basalt weathering in a soil mesocosm without plants and found that the combined application of basalt and *B. subtilis* showed higher CDR potential compared to basalt-only application. In a 99-day mesocosm study, Vienne et al. (2022) observed significant increases in soil cation exchange capacity (CEC), as well as Ca^{2+} and Mg^{2+} levels, following basalt amendment. Furthermore, a 4-year large-scale field trial conducted by Beerling et al. (2024) demonstrated that basalt-induced enhanced weathering not only improved soil health but also potentially contributed to CDR, leading to increased maize and soybean yields. In this study, we demonstrate at three different experimental scales that *Bacillus subtilis* strain MP1 accelerates silicate weathering and promotes the formation of SIC leading to CO_2 removal in agricultural soils. First, we show that MP1 effectively dissolves silicates, facilitating carbonate precipitation in vitro. This finding is further supported by observations from both mesocosm experiments and field trials, where we detected increased SIC formation and evidence of accelerated silicate weathering following MP1 application. Overall, MP1 was shown to be effective in promoting SIC formation across all three experimental settings.

Our research highlights the possibility of boosting native silicate weathering and SIC formation in agricultural soils using microorganisms. This approach can draw down atmospheric CO_2, thereby playing a role in addressing climate change. To our knowledge, this is the first demonstration that a microbial inoculum applied in the field can increase SIC content. Future studies will determine whether our findings are applicable to various field types with different soil pH and across different geographical regions.

2 | Materials and Methods

2.1 | Isolation and Identification of Strain MP1

Bacillus subtilis strain MP1 is a naturally occurring soil microbe isolated from corn roots and rhizospheric soil samples from Santa Barbara County, California, USA. Root samples with rhizospheric soil attached were collected and stored in a clean plastic bag. Soil and roots were divided into two samples (roots and rhizospheric soil) and portions of each sample were plated on LB-Lennox agar medium (10 g L^{-1} tryptone, 5 g L^{-1} yeast extract, 5 g L^{-1} NaCl, 15 g L^{-1} agar). MP1 was recovered as colonies from both samples, rhizospheric soil and roots.

Macrogen Inc. (South Korea) performed genome sequencing and assembly of the MP1 isolate using both PacBio and Illumina reads, and the resulting assembled genome was annotated with Bakta (Schwengers et al. 2021). Taxonomic classification of the strain was performed in three steps. First, 16S rRNA analysis of the MP1 strain against the prokaryotic 16S database (Quast et al. 2012) determined the strain to be of the *Bacillus* genus. Second, whole genome alignment against NCBI *Bacillus* reference genomes using mummer (Marçais et al. 2018) revealed > 90% similarity to *B. subtilis* reference strain (NCBI taxonomy ID = 224308). Third, a deeper whole genome alignment with all complete *B. subtilis* genomes in NCBI showed MP1 to have 99% nucleotide similarity with isolate *B. subtilis* NRS6181B (NCBI Refseq GCF_905318255.2), recorded in a previous exploration of biofilm-producing *B. subtilis* isolates (Kalamara et al. 2021).

2.2 | Strain Growth Conditions

Strain MP1 was routinely cultured at 30°C in LB-Lennox medium or B4 medium (4 g L^{-1} yeast extract, 5 g L^{-1} dextrose, pH adjusted to 8.2 with NaOH) supplemented with 5 g L^{-1} tryptone, termed B4+ medium for this work (Boquet et al. 1973; Sezonov et al. 2007). Agar was added to a final concentration of 15 g L^{-1} for solid preparations. To study silicate weathering in vitro, B4+ medium was supplemented with a plagioclase silicate rock (VWR). Plagioclase feldspars are calcium- and sodium-containing aluminum-silicate minerals that form a solid solution series comprising albite ($Na(AlSi_3O_8)$) and anorthite ($Ca(Al_2Si_2O_8)$) minerals (Okrusch and Frimmel 2020). The silicate rock was ground and sieved through a #10 mesh and captured by a #60 mesh to obtain a particle size ranging from 0.25 to 2 mm. The ground rock was autoclaved at 15 psi for 20 min on a rapid exhaust cycle and dried at 70°C overnight. 300 mg of ground rock was added to B4+ medium at pH 8.8 for in vitro weathering experiments. To confirm the mineral composition of the silicate rock, samples of the ground rock were also submitted to the Department of Earth and Planetary Sciences at the University of California, Berkeley, for X-ray diffraction (XRD) analysis on a Panalytical X'Pert Pro instrument. This analysis

showed that the ground silicate rock was primarily labradorite, a calcium-enriched plagioclase feldspar. In addition, magnesium iron silicate was detected as well.

2.3 | In Vitro Silicate Weathering Assay Conditions and Analysis

To study MP1's ability to accelerate silicate dissolution in vitro, a 7-day time course experiment was performed as follows. Three milliliters of liquid B4+ medium with or without 200 mg ground silicate was inoculated at a final OD_{600} of 0.1 in triplicate from an overnight culture of strain MP1 in 22 mL gas chromatography glass vials (Thermo Scientific), sealed with a breathable membrane (Diversified Biotech, Breathe-EASIER tube membranes), and incubated without shaking at 30°C for 0, 1, 2, 5, and 7 days.

Calcium and magnesium were quantified using a method that relies on the reaction of *o*-cresolphthalein complexone (oCPC) with Ca^{2+} and Mg^{2+} ions in an alkaline solution to form an intense violet-colored complex that maximally absorbs at 577 nm (Connerty and Briggs 1966; Moorehead and Biggs 1974). To quantify Ca^{2+} and Mg^{2+} in solution, 500 μL of supernatant was removed from cultures (three biological replicates) at different time points and pelleted to remove debris. Twenty microliters of the clarified supernatants was combined with 180 μL oCPC resuspended in Tris–HCl, pH 8.3 to a final concentration of 85 μM and 5 mM, respectively. To quantify inorganic carbon formation, calcium carbonate equivalent (CCE, which incorporates both solid-phase carbonates and dissolved inorganic carbon) was determined by gas chromatography (GC), as described below. pH was measured in liquid culture samples using an Orion Versa Star Pro (Thermo Scientific) pH meter.

2.4 | Calcium Carbonate Equivalent Determination Using Gas Chromatography

To quantify inorganic carbon formation, GC glass vials (Thermo Scientific) containing standards or experimental samples (i.e., from in vitro weathering or mesocosm experiments) were capped, and 2 mL 4 N H_2SO_4 (Ricca Chemical) plus 3% (w/v) $FeSO_4 \cdot 4H_2O$ (to inhibit the release of CO_2 from organic matter) was injected through the septum in the cap into each vial. Vials were incubated at room temperature for at least 2 h to evolve CO_2 from all inorganic carbon species in the sample. The headspace of each vial was analyzed for CO_2 content by GC. 1 mL headspace was sampled by autosampler and analyzed on a Thermo Scientific TRACE 1310 GC fitted with a thermal conductivity detector (Thermo Scientific 1300 IN Series) and capillary column (Restek RT-Q-Bond PLOT). The GC column flow rate was 9.8 mL min^{-1} with a split ratio of 10, using helium as a carrier gas. This process measures the CO_2 released from carbonate minerals (both formed on the biofilm and precipitated to the bottom of the vial) and any ions in solution (i.e., bicarbonate and carbonate ions). A standard curve was prepared using known amounts of $CaCO_3$, and experimental values were expressed as CCE. The area under the CO_2-specific peak was determined using Chromeleon 7 software (Thermo Scientific) and fitted to the $CaCO_3/CO_2$ standard curve to calculate CCE. Details of the GC method can be found in Yip et al. (2025).

2.5 | Mesocosm Study Setup and Analysis

For the mesocosm study, the soil was obtained from Richmond, CA (American Soil & Stone). Henceforth, this soil is referred to as SBX15. The chemical and physical properties of SBX15 are provided in Table S1. Notably, the mineral fraction of SBX15 comprised 40%–45% feldspar minerals (Table S1). For the mesocosm study, approximately 50 kg of SBX15 soil was manually homogenized with shovels. Columns (30.5 cm in height and 10 cm in diameter) were packed with 3.1 kg of SBX15 soil. The experiment comprised two groups, MP1 and untreated control (UTC), with six replicate columns in each group. One seed of dent corn (hybrid Integra Corn 5802 VT2Pro) was sown per column (Figure 2a, Figure S3a). For MP1 treatment, each seed was inoculated with 1.4×10^6 MP1 spores by applying 1 mL of a liquid solution containing MP1 at a concentration of 1.4×10^6 spores mL^{-1} and distilled water as the carrier. Each seed from the UTC received 1 mL of distilled water. The experiment was conducted in a growth chamber, and the growing conditions were as follows: the temperature was set at 22°C (±5°C), with a relative humidity of 65% (±5%) and a photoperiod of 16 h. Plants were watered two times per week for the first 6 weeks. We simulated a period with rainfall the following 2 weeks using deionized water containing approximately 738 ppm CO_2 (carbonated water). The simulated amount of rainfall was calculated based on historical precipitation data (from 2017 to 2021) retrieved from a weather station operated by the National Oceanic and Atmospheric Administration (NOAA NCEI 2024), located 17 km away from the field trial site. This translated into 1.75 L of water per column, divided into eight rainfall events (218.8 mL per event) during the 2 weeks. The cadence of the rainfall was 2 days, followed by 2 days without rainfall until 8 total days of rainfall were reached. Leachate was collected from each column during the eight rainfall events to account for the flux of compounds leaving the column with the leachate. After the 2-week rainfall period, the plants were allowed to grow for an additional week before harvesting.

After 9 weeks, each of the 12 columns was harvested, and soil samples were collected at three depths (0–10, 10–20, and 20–30 cm; Figure S3), resulting in a total of 36 samples. Soil bicarbonate and carbonate ions were determined using a saturated paste extract followed by titration, as detailed in Supporting Information and Richards (1954). In brief, 200 g of dried and sieved soil (particle size < 2 mm) was used to prepare a saturated soil paste, and the 10 mL soil saturation extract with 0.025 N H_2SO_4 was titrated using phenolphthalein and methyl orange as indicators to quantify bicarbonate and carbonate ions.

One hundred grams of each soil sample was sent to an external commercial laboratory (Agvise Laboratories, ND, USA) to quantify the following: pH, organic matter, exchangeable calcium, exchangeable magnesium, exchangeable potassium, exchangeable sodium, exchangeable iron, total aluminum, and total carbon. Soil pH was determined by the 1:1 soil/water method using a pH meter (Peters et al. 2012), and soil organic matter was determined by the loss of ignition at 360°C (Combs and Nathan 1998). Soil exchangeable calcium, magnesium, potassium, and sodium were extracted using a 1 M ammonium acetate (NH_4OAc) solution at pH 7, and their concentrations were determined by inductively coupled plasma atomic

emission spectrometry (ICP-AES; Perkin Elmer Optima 5300, Optima 7300—Warnacke and Brown 2015). Exchangeable iron was extracted using a DTPA-TEA (diethylenetriaminepentaacetic acid—triethanolamine) solution and measured by ICP-AES (Whitney 2015).

Total aluminum was extracted by treating 0.25 g of dried, sieved soil with concentrated HNO_3, 30% H_2O_2, and concentrated HCl using the EPA method (EPA U.S. 1996). This procedure effectively dissolves materials that may become environmentally available, such as carbonate, phosphate, and sulfate minerals, while not breaking down resistant silicates. Aluminum in the extract was quantified using ICP-AES (Perkin Elmer Optima 5300, Optima 7300, and Avio 500 Max series). Soil total carbon was quantified by the combustion method using the vario MACRO cube elemental analyzer (Elementar Americas Inc., NY), and total organic carbon is equal to total carbon minus total inorganic carbon determined by CCE (Nelson and Sommers 1996). The individual leachate samples, collected from each column during the eight rainfall events, were sent to Agvise to analyze pH, soluble calcium, soluble magnesium, soluble potassium, soluble sodium, and soluble iron (American Public Health Association 1926). Bicarbonate and carbonate ions were quantified by titration with 0.025 N H_2SO_4 with phenolphthalein and methyl orange indicators (Richards 1954). CCE from soils and leachates was measured using the GC method detailed in the previous section.

2.6 | Soil Mineral Composition Determination

The mineral composition of the soil used in the mesocosm study (SBX15) and soil samples from the field study was obtained by a combination of the scanning electron microscope (SEM) observations on a Zeiss EVO-10 Variable Vacuum SEM and XRD analysis with the PANalytical X'Pert Pro diffractometer at the Department of Earth and Planetary Science at the University of California, Berkeley. Approximately 0.3 g of ground soil samples (six UTC fields and eight MP1-treated fields) were plated via a fast-drying acetone mixture for XRD. A subset of nine soil samples was analyzed under SEM (four UTC fields and five MP1-treated fields). Before SEM analysis, a separate ~0.3 g fraction of ground soil was mixed with ~40 mL of deionized water and sonicated to remove clay particles from grains and into suspension. The clay-water solution was decanted, and the remaining mineral grains were dried in an oven for 20 min at ~40°C. XRD results are coupled with these SEM observations to provide a quantitative approximation of the bulk mineral composition of the soil sample and corroborate percentages provided by SEM grain counting.

2.7 | MP1 Application as a Seed Treatment for Field Study

Soybean seeds were overcoated with a formulation that contains fungicides, insecticides, and *B. subtilis* strain MP1. Untreated control seeds for UTC fields were overcoated with the same formulation of fungicides and insecticides but without MP1. MP1 application rate was 37 mL per hectare (0.5 fl oz./acre) of a formulation containing deionized water and MP1 spores at a concentration of 5.0×10^{10} spores mL^{-1}. Each soybean seed was covered with approximately 5.0×10^6 spores of strain MP1.

2.8 | Field Study Setup and Sample Collection

A large-scale field study was conducted in Stutsman County, North Dakota, USA in 2022 on 14 soybean fields, eight MP1-treated fields, and six UTC fields. The total extension of the field study comprised 847 ha. All the fields were located within a radius of 18.2 km of each other. They were all watered by rainfall, without additional ground or surface water irrigation, with a mean accumulated 2022 precipitation of 472.9 mm (NOAA NCEI 2024). The fields used in this study did not receive limestone application 10 years before the field trial.

According to the USGS North American Soil Geochemical Landscapes database, the total feldspar in the soil A horizon in this region ranges between 17.7 and 27.5 wt% (Smith et al. 2019). The overall mineral composition of these fields (Figure S5) was determined as described in a previous section of Section 2.

Each field was stratified based on soil texture considering the first 30.5 cm (12 in.) of soil (data retrieved from the USDA NRCS 2024 SSURGO database), and three to five sampling locations per stratum were selected. Samples were collected before planting, at the beginning of May (henceforth pre-planting), and after harvest (henceforth post-harvest), approximately in mid-October. Each collected sample was made up of soil composites comprising 10 core samples from the top 30.5 cm (12 in.) of soil collected in a radius of 3 m from the center point. The center points were defined by an algorithm that randomly selected points within each stratum, and coordinates were recorded to return to the exact location post-harvest. For the soybean fields, 47 sampling locations (23 MP1 and 24 UTC) were used across the MP1-treated fields and UTC fields. The soil composites were homogenized and subsamples were sent to Agvise Laboratories. Dried, ground, and sieved (2 mm) soil samples were used for all soil analyses. Agvise determined CCE, total carbon, soil pH, exchangeable calcium, and cation exchange capacity (CEC). CCE was measured by the modified pressure-calcimeter method described in Sherrod et al. (2002). In brief, 2 g of soil was placed into a 35 mL plastic cup and transferred into a 236 mL glass jar. The glass jar is secured and sealed with a lid and rubber gasket. A dispensing pump added 10 mL of 4.6 M HCl plus 3% (w/v) of $FeCl_2 \cdot 4H_2O$ into the glass jar. The jar was incubated for 20 min in a shaker at 180 rpm and then the pressure was recorded in volts in a pressure transducer (26 PC series, Honeywell, MN). Soil CEC was determined by the ammonium acetate (pH 7) method described in Sumner and Miller (1996), which involves saturation with 1 M NH_4OAc at pH 7, three rinses with 95% ethanol, and a final rinse with 1 M KCl. Details about the total carbon, soil pH, and exchangeable calcium analysis can be found in the mesocosm study setup and analysis section and Supporting Information.

2.9 | Statistical Analyses

Shapiro–Wilk tests were conducted to assess whether the data sets have a normal distribution. Additionally, F tests were

conducted to assess the homogeneity of variance between the treatment and control groups.

With a normal distribution of the data and homoscedasticity, an unpaired *t*-test was conducted to analyze the results shown in Figure 1c,d. Otherwise, a Mann–Whitney test was conducted. For Figure 1c, asterisks indicate statistically significant differences among MP1 and MP1 + feldspar treatments within a specific time point ($n = 3$ per group per time point). For Figure 1d, asterisks indicate statistically significant differences among medium + feldspar and MP1 + feldspar treatments within a specific time point ($n = 3$ per group per time point). The results in Figure 1e were analyzed using a two-way ANOVA followed by Tukey's multiple comparisons test, while those in Figure 1f were analyzed using a one-way ANOVA with Tukey's test. Different letters on the bars indicate statistically significant differences among treatments ($n = 3$, p-value < 0.05).

Unpaired *t*-tests were conducted after confirming normal distribution and homogeneity of variance in the datasets to statistically analyze the differences between UTC and MP1 in the mesocosm study (Figure 2) and the field study (Figure 3). The Welch *t*-test was applied when the homogeneity of variance criteria were not met. Six biological replicates were used for the mesocosm study, while 23 biological replicates for MP1 and 24 biological replicates for UTC were used for the field study.

For all the figures with asterisks, one asterisk represents a p-value < 0.05, two asterisks represent a p-value < 0.01, three asterisks represent a p-value < 0.001, and four asterisks represent a p-value < 0.0001.

3 | Results and Discussion

3.1 | MP1 Promotes Silicate Dissolution and Carbonate Precipitation In Vitro

Various soil microorganisms have been reported to enhance the dissolution of minerals, including silicates (Liu et al. 2006; Sheng et al. 2008). We set out to investigate if the *Bacillus subtilis* strain MP1 is able to accelerate silicate dissolution as well. To determine the extent by which MP1 can extract cations from silicates, we grew MP1 in liquid B4+ medium over a 7-day period in the presence or absence of Ca-bearing feldspar and monitored the release of Ca^{2+} and Mg^{2+} in the cultures. In uninoculated cultures with feldspar, we observed some initial release of Ca^{2+} and Mg^{2+} increasing the baseline to ~0.2 mM after day one, which we attribute to the weathering of easily accessible ions from the feldspar by the culturing liquid. In contrast, soluble Ca^{2+} and Mg^{2+} concentrations in MP1 cultures with feldspar increased to ~0.6 mM on days one and two and then dropped back to baseline, below the levels observed in uninoculated cultures supplemented with feldspar (Figure 1d). This is not entirely unexpected, as in cultures supplemented with feldspar, we observed both the formation of a robust biofilm and heat-resistant spores (10^9 spores mL^{-1} at day 7), which are both known to take up Ca^{2+} (Ercole et al. 2012; Kim et al. 2017; Han et al. 2018; Zhuang et al. 2018; Paidhungat et al. 2000; Nishikawa and Kobayashi 2021; Azulay et al. 2022). We confirmed in a highly related strain that removing the ability to sporulate by knocking out the *spoIIE* gene returned the concentration of Ca^{2+} and Mg^{2+} to detected initial levels, indicating a significant amount is consumed in the sporulation process. In addition, we hypothesized that some portion of Ca^{2+} and Mg^{2+} was used in carbonate precipitation, which aligns with the high final pH of the cultures and our previous observations that MP1 can induce carbonate precipitation (Figure 1a,c, respectively).

When grown on solid B4+ medium supplemented with a soluble source of Ca^{2+} (see Supporting Information for details) MP1 promoted calcium carbonate precipitation, as reported for other *Bacillus* strains (Lian et al. 2006; Han et al. 2019), resulting in the accumulation of calcite crystals on the biomass (Figure 1a, Figure S1). We wanted to determine if this carbonate precipitation was also occurring in liquid cultures grown with feldspar by measuring the total inorganic carbon content in the cultures using gas chromatography. This involved comparing the CO_2 released after acid treatment to that of a calcium carbonate standard, expressed as CCE. In MP1 cultures without feldspar, we observed a slight increase in the CCE signal, MP1 cultures with feldspar showed a dramatic increase in CCE (Figure 1e). To establish that the CCE signal was due to elevated levels of Ca^{2+} or Mg^{2+} rather than other ions, we ran similar experiments wherein B4+ medium was supplemented with 25 mM potassium, sodium, magnesium, or calcium acetate instead of feldspar. As expected, the addition of Ca^{2+} or Mg^{2+} acetate resulted in a significantly higher CCE signal compared to control cultures (Figure 1f), suggesting that the elevated levels of Ca^{2+} or Mg^{2+} in solution can lead to carbonate precipitation. In contrast, CCE levels were not altered in the presence of potassium or sodium acetate, indicating the increased signal was not due to the addition of these cations or the metabolism of acetate (Figure 1f). Hence, these results indicate that MP1 is capable of promoting silicate dissolution and that these extracted cations from the minerals can produce biogenic carbonate minerals as an end product.

In the course of these experiments, we observed profound changes in the behavior of the growing cultures, demonstrating the cells are detecting and responding strongly to the substrate. Notably, the addition of feldspar to MP1 cultures induced the production of a robust pellicle biofilm and brown-red pigment (illustrated in Figure 1b) and there was a marked response in pH progression of the culture. In MP1 cultures without feldspar, we observed an initial drop in pH on day one, followed by a gradual increase in pH, with the final pH reaching approximately 8 (Figure 1c). In contrast, in the presence of feldspar, the pH showed a similar initial drop but drastically increased on day 2 compared to MP1 cultures without feldspar (Figure 1c). On days 5 and 7, the pH of cultures with feldspar measured approximately 1 pH unit higher than cultures without feldspar (Figure 1c). Together, these results lead us to hypothesize that the metabolism of growing cells causes a dramatic shift in pH in these in vitro cultures, weathering the feldspar when in the low pH range and releasing metal ions and alkalinity from the mineral, leading to a significant increase in pH that stabilizes at pH 9. Under these conditions, the precipitation of solid carbonates, such as calcite ($CaCO_3$), magnesite ($MgCO_3$) or dolomite ($CaMg(CO_3)_2$) is highly favored. While it is likely that these behaviors are greatly accelerated in these in vitro conditions, these experiments demonstrate that MP1 promotes silicate dissolution and extracts cations from these minerals, yielding biogenic carbonate minerals as an end product. We next demonstrated that these behaviors are also possible in soil with agricultural crops present.

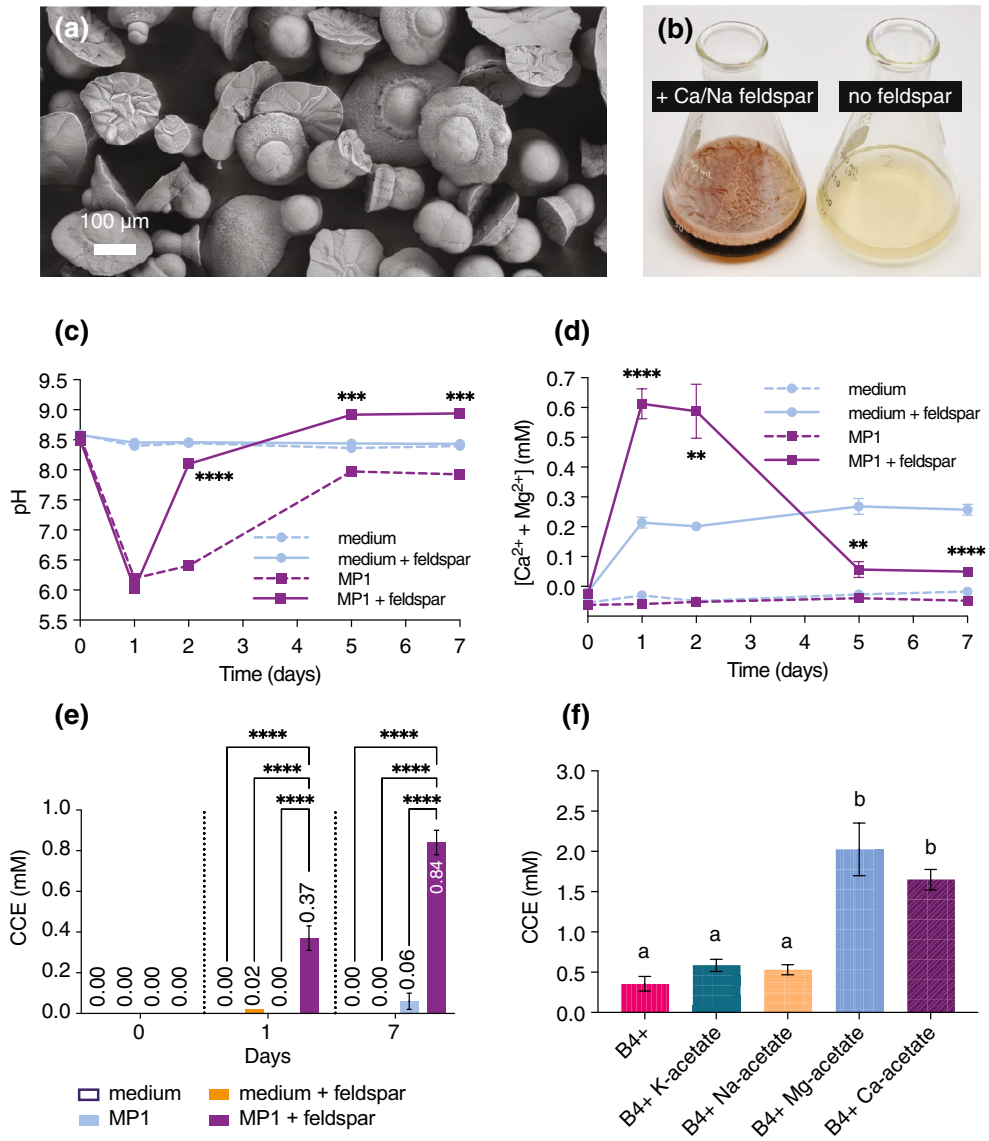

FIGURE 1 | MP1 mediates silicate weathering and carbonate precipitation in vitro. (a) SEM image of calcite crystals isolated from MP1 colonies. (b) Floating pellicle biofilm and brown-red pigments produced by MP1 in the presence of feldspar (left). No pigment and only a thin biofilm were observed in the absence of feldspar after 7 days (right). (c) pH dynamics and (d) $Ca^{2+} + Mg^{2+}$ concentration in solution during a 7-day time course in B4+ medium inoculated with MP1 in the absence or presence of feldspar. Medium with (solid lines) or without (dashed lines) feldspar added was inoculated with MP1 (purple square) or not inoculated (light blue circle), and samples were collected for measurements at days 0, 1, 2, 5, and 7. Each point represents the average of three biological replicates and its standard error. (e) Inorganic carbon expressed as calcium carbonate equivalent (CCE). Measurements were performed at day 0 (orange bars), 1 (light blue bars), and 7 (purple bars) from MP1 and uninoculated cultures. An unpaired *t*-test was conducted for days 1 and 7. The asterisks (*) indicate statistically significant differences between the MP1 and MP1 + feldspar treatments (**p-value < 0.01 and ***p-value < 0.001). (f) CCE measured on day 7 in MP1 cultures in B4+ medium and B4+ medium supplemented with potassium, sodium, magnesium, or calcium acetate. Each bar represents the average of three biological replicates and its standard error. Letters (a or b) above each bar indicate statistically significant differences among the treatments (p-value < 0.05).

3.2 | MP1 Enhances Silicate Weathering Rates and Promotes Soil Inorganic Carbon Formation in Mesocosms

We first established that MP1 can effectively colonize the rhizospheres of corn plants in both growth chamber and greenhouse experiments (Figure S2). We next quantified the ability of MP1 to accelerate the silicate-to-carbonate transition in a 9-week mesocosm experiment with corn, using field soil with a high natural abundance of cation-bearing silicates (Figure S3a, Table S1). Additionally, to mimic field conditions and monitor the mobility of SIC, dissolved inorganic carbon (DIC), and cations, we simulated rainfall events between weeks 6–8 of the experiment and collected leachates from the columns.

After 9 weeks, we observed a ~20% increase in the inorganic carbon content (measured as CCE) in the overall system (soil plus leachate) in MP1-treated columns compared to the untreated control (UTC) columns (Figure 2b, Figure S3b), underscoring the ability of MP1 to promote SIC buildup. Moreover, we

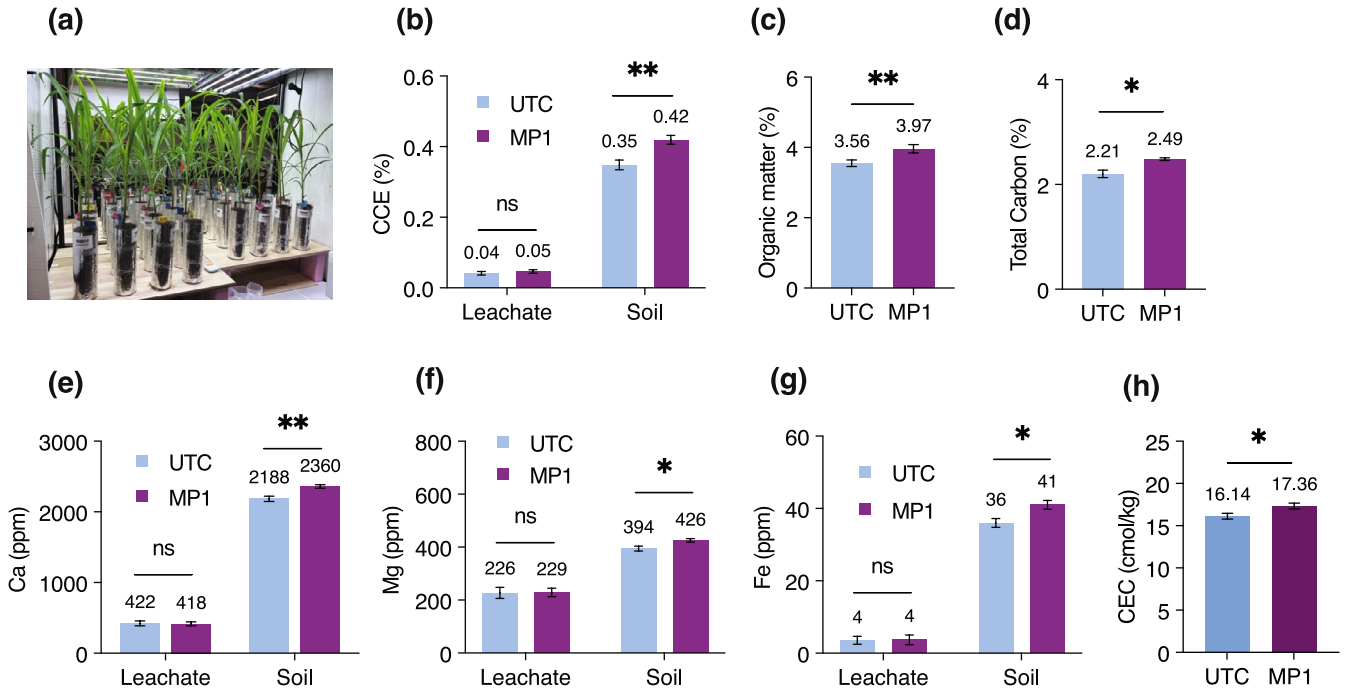

FIGURE 2 | MP1 promotes soil inorganic carbon formation and increases soil fertility. (a) Image of the mesocosm setup with 7-week-old corn plants. (b) Soil inorganic carbon (SIC) is measured as calcium carbonate equivalent (CCE) in the leachate and soil. (c) Organic matter and (d) total carbon on MP1 and untreated control (UTC) soils. (e) Exchangeable calcium, (f) exchangeable magnesium, and (g) exchangeable iron were measured in MP1 and UTC soils, and the same cations were measured as soluble cations in MP1 and UTC's leachates. The *y*-axis shows cation concentration in ppm. For the leachate results, ppm represents milligrams per liter of leachate, whereas for the soil results, ppm represents milligrams per kilogram of soil. (h) Cation exchange capacity (CEC) on MP1 and UTC soils. For (b)–(h), each bar represents the average of six biological replicates and its standard error. The asterisks (*) indicate statistically significant differences against UTC (*p-value < 0.05 and **p-value < 0.01).

observed an increase in organic matter (~12%) and total carbon content (~13%) in MP1-treated columns compared to UTC columns (Figure 2c,d), while the final soil and leachate pH were similar for MP1 and UTC (Figure S4d). Additionally, we observed statistically significantly higher DIC in MP1-treated soils in comparison to UTC soils (Figure S4f), while a slight increase in favor of MP1 treatment was found in the DIC from the leachates (Figure S4e). Given the soil and leachate pH (> 8.1), we speculate that bicarbonate and carbonate ions would constitute most of the DIC species. Since the formation of carbonates requires cations, we measured concentrations of available cations in the exchangeable and soluble pools in the soil and leachate samples, respectively. We observed a statistically significant increase in exchangeable Ca^{2+}, exchangeable Mg^{2+} and $Fe^{2+/3+}$, and CEC in MP1-treated columns (Figure 2e–h, Figure S3c,d,h) compared to UTC columns. Additionally, we observed a smaller increase in exchangeable Na^{+} and K^{+} in MP1-treated soils (Figures S3e,g and S4a,b). Furthermore, we measured extractable Al in the soil as one of the major structural elements of silicates. The method for aluminum extraction used in this study quantified aluminum in carbonates, phosphate, and sulfate minerals, and organic compounds and did not extract aluminum from silicates (as would be the case for hydrofluoric acid extraction). We found that extractable Al levels increased in MP1-treated soils compared to UTC soils (Figures S3f and S4c). Together, these results support a model wherein MP1 can accelerate native silicate dissolution and extract cations. At the same time, MP1 promotes SIC formation, taking advantage of the elevated levels of available calcium, magnesium, and iron.

Finally, we calculated the native silicate weathering and carbonate precipitation rates for MP1 and UTC over the course of the experiment (63 days) using the measurements for exchangeable calcium ($Ca^{exchangeable}$), total inorganic carbon (CCE), and DIC content in soil and leachate fractions (see Supporting Information for details). Our calculations showed that MP1-treated soils had a notably higher native silicate weathering rate (13.24 ± 4.34 mmol kg $soil^{-1}$ versus 1.96 ± 4.31 mmol kg $soil^{-1}$) and carbonate precipitation rate (5.33 ± 1.44 mmol kg $soil^{-1}$ versus -1.58 ± 1.34 mmol kg $soil^{-1}$) as compared to untreated control soils. Assuming an average specific surface area of 1.13 $m^2 g^{-1}$ anorthite (te Pas et al. 2023), the specific weathering rate of anorthite particles estimated for MP1-treated soil is 5^{-12} mol $m^{-2} s^{-1}$. While this is an approximate estimate based on an assumed mineral surface area, it is noteworthy that this rate is at the higher end of the known bounds of natural feldspar weathering rates from field studies reported in literature (White and Brantley 2003; Gruber et al. 2014; Wild et al. 2021). Consequently, MP1 is estimated to have a net CO_2 removal rate of 7.60 ± 1.22 mmol kg $soil^{-1}$ higher than the untreated control over the course of the experiment, which translates to a net sequestration of 0.39 ± 0.06 tonnes inorganic C ha^{-1} (see Supporting Information for details). Notably, the net sequestration of inorganic carbon by MP1 was between that observed in a field experiment with varying levels of wollastonite application, which sequestered between 0.13 and 0.65 tonnes of inorganic carbon per hectare (Xu et al. 2024). Numerous factors, such as rock type, dosage, composition of feedstock, the type of experiment (e.g., lab experiment, field trial, or modeling), the timeframe of

the measurements (weeks, months, or years), and methods for quantifying CDR, can influence CDR rates and lead to significant variability across studies (Power et al. 2025). To the best of our knowledge, studies investigating the enhancement of weathering rates typically require extended periods, such as the 99-day mesocosm study by Vienne et al. (2022), a 129-day mesocosm study by Niron et al. (2024), a 235-day mesocosm study by Reershemius et al. (2023), a 2-year field experiment by Xu et al. (2024), and a field trial spanning over 4 years by Beerling et al. (2024). In contrast to these previous studies, we observed a weathering rate of native silicates of 0.39 ± 0.06 tonnes of inorganic carbon per hectare within 63 days. The higher observed weathering rate and SIC formation could be explained by the elevated content of native silicates present in the soil used in this study (40%–45% feldspar minerals—Table S1). Taken together, our results demonstrate that MP1 not only accelerated the weathering of native silicates in the soil but also promoted the formation of SIC, thereby removing CO_2 from the atmosphere.

3.3 | MP1 Promotes Soil Inorganic Carbon Formation and Replenishes Calcium in the Field

To evaluate MP1 performance under field conditions, we carried out a large-scale field trial in 2022. We applied MP1 as a seed treatment on eight soybean fields located in North Dakota (USA). The field study also comprised six untreated control (UTC) fields (i.e., fields without MP1) in the same area. We performed extensive soil sampling pre-planting and post-harvest to assess the impact of MP1 on SIC and several other soil key characteristics. SIC (measured as CCE) in the top 30.5 cm (12 in.) increased during the season (from pre-plant to post-harvest). We observed a significant increase in the ΔCCE on the MP1-treated fields as compared to the untreated fields (0.57% ± 0.17% versus 0.15% ± 0.10%, respectively) (Figure 3a). This increase in CCE (ΔCCE MP1 − ΔCCE UTC) equates to approximately 2.02 tonnes C ha^{-1} $year^{-1}$ gross inorganic carbon accrual, assuming an average soil bulk density of 1.33 g cm^{-3} ± 0.07 (USDA NRCS 2024 SSURGO database), 0.305 m sampling depth, and the molecular weight conversion from calcium carbonate to carbon (i.e., 0.12). This calculation should be considered an upper limit on CO_2 removal potential given that observed net changes in the field soil may have been driven by cations derived from non-silicate sources. We also observed an improvement in total carbon on MP1-treated fields (0.21% ± 0.04%) compared to UTC fields (0.13% ± 0.04%; Figure 3b). Most of this increase is explained by the inorganic carbon component as the total organic carbon concentration showed little difference between MP1-treated (0.15% ± 0.05%) and UTC (0.14% ± 0.04%) fields. We observed a minor decrease in exchangeable calcium in MP1-treated fields, while a clear decrease was observed in UTC fields (Figure 3c), the

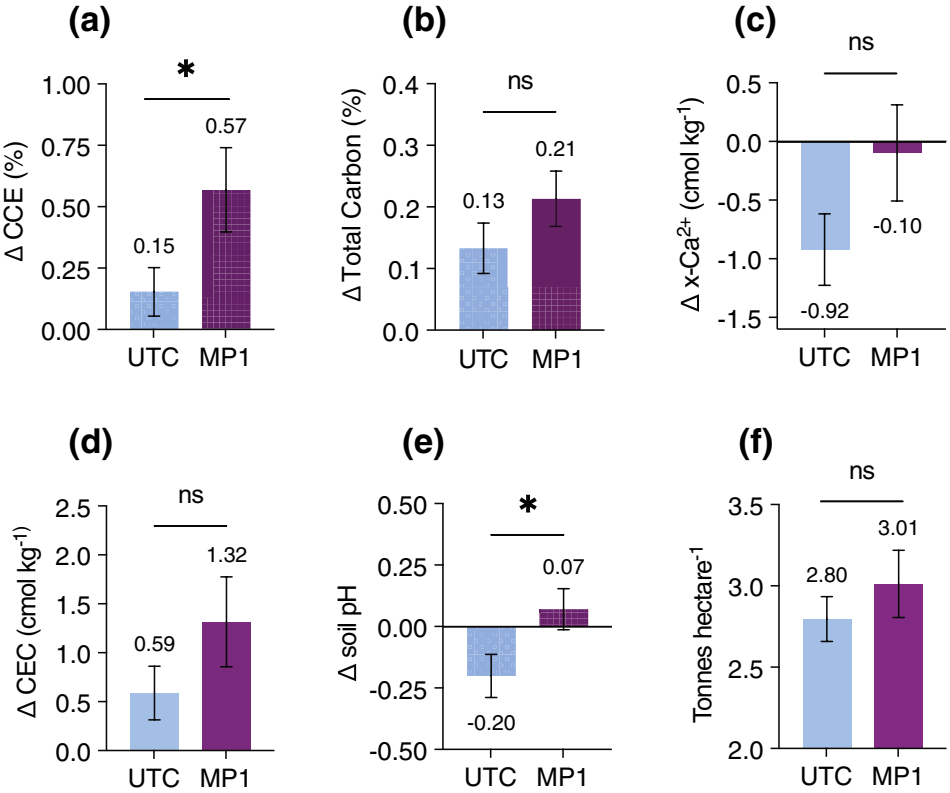

FIGURE 3 | MP1 field application increases soil carbon and positively affects soybean yield. (a) Inorganic carbon formation (measured as calcium carbonate equivalent, CCE). (b) Total carbon changes, (c) exchangeable calcium changes, (d) cation exchange capacity (CEC) changes, and (e) soil pH changes during the 2022 growing season on soybean fields. Each bar represents the average change between pre-plant and post-harvest on untreated control (UTC) fields and MP1-treated fields. For all the soil results (a–e), the bars represent the average of 24 sampling points taken from six UTC fields and 23 sampling points taken from eight MP1-treated fields and their standard error. (f) Soybean grain yield from 12 fields in North Dakota in the 2022 growing season. The MP1 bar represents the average of seven treated fields and its standard error, and the UTC bar represents the average of five untreated fields and its standard error. The asterisks (*) indicate statistically significant differences against UTC (*p-value < 0.05).

delta between the two groups being 0.82 cmol kg^{-1} (unpaired *t*-test, *p*-value = 0.10). Additionally, we observed an increase of 1.32 ± 0.46 cmol kg^{-1} in the cation exchange capacity on MP1-treated fields compared to 0.59 ± 0.27 cmol kg^{-1} for UTC fields (Figure 3d). In rock weathering studies, an increase in CEC can possibly be explained by an increase in secondary clay minerals, a byproduct of silicate weathering (Vienne et al. 2022). Due to microbial and plant metabolism, soils tend to acidify during the growing season (Marschner 2011). This phenomenon is observed in UTC fields where the drop in pH throughout the season was 0.20 units (Figure 3e). However, the soil pH on MP1-treated fields increased by 0.07 units in the same period (Figure 3e). Importantly, MP1 also positively affected yield in this field study, with an average grain yield increase of 0.21 tonnes ha^{-1} compared to UTC fields (Figure 3f), a 7.5% improvement over UTC. Consistent with the in vitro and mesocosm results, our field study supports the notion that MP1 enhances silicate weathering rates and SIC formation over one agricultural growing season.

3.4 | Microbially Mediated Carbon Sequestration in Soils

We have demonstrated that a targeted application of a microbial soil treatment can accelerate native silicate weathering and promote inorganic carbon formation within one agricultural season. MP1 accelerated silicate dissolution in vitro and used the extracted cations to promote carbonate precipitation (Figure 1). In agreement with these observations, we observed the formation of SIC and higher levels of readily extractable cations in the soil after MP1 treatment in controlled mesocosm and field studies (Figures 2 and 3). Our findings suggest that MP1 targets silicates naturally present in the soil (Figure S5), and that carbonate precipitation mediated by MP1 facilitates the weathering of these native silicates. In the agroecosystem where we conducted the field trial, the amount of total feldspar in the soil A horizon ranged between 17.7 and 27.5 wt% (Smith et al. 2019), levels that are similar to many soils around the globe where primary silicate minerals are also naturally abundant (Hartmann and Moosdorf 2012). Accelerated weathering of these native silicates has the potential to enhance soil fertility and promote carbon dioxide removal via SIC formation. In addition to the SIC formation, the elevated calcium and iron availability associated with MP1 treatment may also promote soil organic carbon persistence through the formation of mineral-associated organic matter (MAOM) mediated by physicochemical and biotic processes (Rowley et al. 2018; Shabtai et al. 2023; Bramble et al. 2024). Further studies can be performed to assess the impact on MAOM formation by MP1 in agricultural soils.

Although the exact mechanism for silicate weathering by MP1 is unknown, microorganisms have been reported to enhance mineral weathering by impacting important kinetic parameters through the production of protons mediated by carbonic anhydrases (CAs) (Xiao et al. 2015; Vicca et al. 2022), organic and inorganic acids (Frey et al. 2010), secretion of chelating agents or redox-active molecules (Kraemer 2004; Newman and Kolter 2000; Lee et al. 2012), and attachment to mineral surfaces (Ahmed and Holmström 2015). MP1 produced a robust biofilm and brown-red pigment in the presence of silicates in vitro. Furthermore, the presence of silicates altered the pH profile of MP1 cultures (Figure 1). Bacterial biofilms have been proposed to play an important role in mineral dissolution by facilitating adherence to rock surfaces and concentrating weathering agents (Han et al. 2024; Finlay et al. 2020; Kemmling et al. 2004). In addition to acid production (observed by the initial drop in culture pH—Figure 1c), our results point to the possible role of chelation in MP1-mediated weathering. First, the negatively charged extracellular matrix of *Bacillus* biofilms can serve as a binding site for cations such as Ca^{2+} (Ercole et al. 2012; Kim et al. 2017; Han et al. 2018; Zhuang et al. 2018). Second, the brown-red pigment

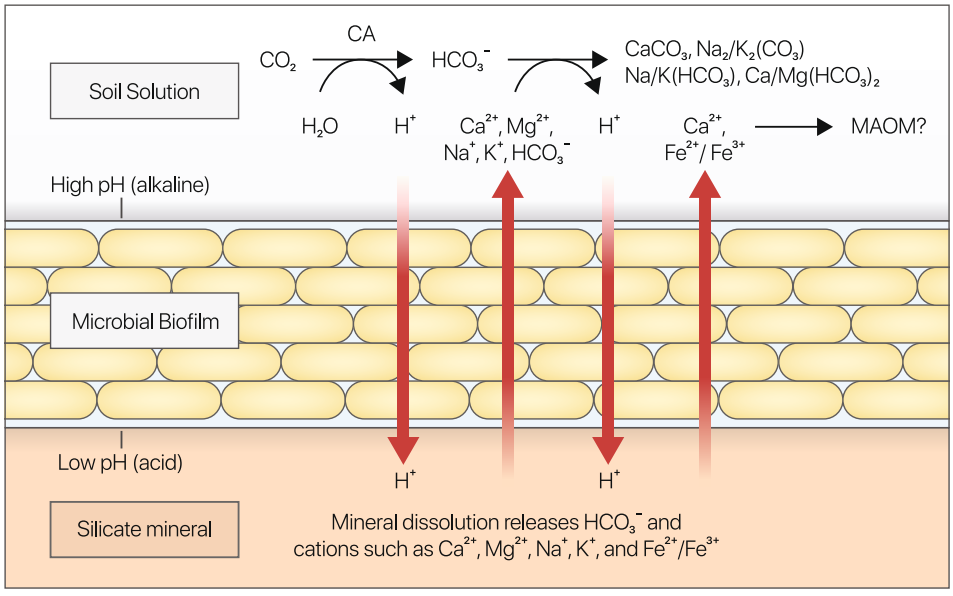

FIGURE 4 | Proposed model by which MP1 promotes inorganic carbon formation in the soil. We hypothesized that MP1 forms a biofilm on the surface of silicate minerals. At the mineral surface-biofilm interface, MP1 regulates the transport of ions (i.e., protons and cations) to generate a low pH microenvironment at the mineral–biofilm surface and a high pH and high cation concentration microenvironment at the biofilm-bulk solution interface. This physically separates the silicate weathering process from soil inorganic carbon formation, including carbonate precipitation.

(Figure 1b) is reminiscent of an iron chelator, pulcherrimin, for which MP1 carries the genes (Arnaouteli et al. 2019). These observations support a model wherein MP1 senses the presence of cation-bearing silicates and forms a biofilm to colonize the mineral surface and alter chemical conditions at the mineral-biofilm interface. While maintaining an optimal microenvironment for silicate dissolution at the mineral-biofilm interface, we hypothesize that SIC formation, including carbonate precipitation, is promoted at the interface with the bulk soil (Figure 4). The proposed model is consistent with a 'trans' calcification type model described by McConnaughey and Whelan (1997). In lab experiments, we observed a steep increase in the pH of MP1 cultures facilitating carbonate precipitation (Figure 1c,e). We also observed a statistically significant difference in the average change of soil pH of MP1-treated soils compared to untreated soils in our large-scale field study (Figure 3e). This could be explained by a multifactorial effect in which protons generated by the hydration of CO_2 are directed and concentrated toward the silicate minerals through MP1 biofilm, with the silicate minerals acting as a sink for these protons (Figure 4). This process, in turn, promotes the dissolution of the silicates. Consequently, base cations and bicarbonate are released to the soil solution (Figure 4). A portion of the base cations may displace protons from the soil exchangeable sites, further increasing the soil pH.

Overall, our data suggest that silicate weathering, increased cation availability, and pH modulation of the bulk solution are key mechanisms driving the increase in the SIC evidenced in this study.

4 | Implications and Future Perspective

Agricultural practices can fundamentally alter the inorganic carbon cycle in soils (Zamanian and Kuzyakov 2022; Suarez 2000; Lal and Kimble 2000; Sanderman 2012). Due to the massive scale of available arable land globally, agriculture holds the potential to be a major contributor to CDR. For farmers to contribute to CDR, they will need access to solutions compatible with their operations. MP1 application has the potential to be one of such solutions. *Bacillus* spp. have been used as agricultural input products for decades to promote plant growth, enhance nutrient availability, and act as a biocontrol agent for plant diseases and pests (Aloo et al. 2019; Xavier et al. 2023). MP1 application is compatible with standard farm practices and increased the average yield for soybeans in our field trial (Figure 3f). It should be noted that year-on-year MP1 application could result in a reduction of primary silicate minerals over time that could ultimately affect soil fertility. Additional research is needed to estimate how long this approach can sustainably be deployed in various soils. In the field, we estimated a gross accrual of 2.02 tonnes inorganic C ha^{-1} $year^{-1}$ based on the observed 0.42% additional CCE formation for MP1 treatment compared to UTC (Figure 3a). We postulate that most of the CCE formation is attributable to weathering of Ca, Mg, Na, and K-bearing silicates (the latter two resulting in DIC). Second, it is conceivable that MP1 also accelerates the weathering of other cation-bearing, non-carbonate minerals such as phosphates, sulfates, and oxides. Finally, as the field study comprises an open system, the ability of MP1 to affect the retention of cations from atmospheric deposition and fertilizer and its influence on the vertical distribution of naturally occurring soil carbonates needs to be considered. Although the contribution of the latter two processes remains to be determined in the field, it is worth noting that these are ruled out as factors in controlled mesocosm studies. Future studies could incorporate the contribution of MP1 to silicate weathering into established reactive transport models to address vertical distribution, carbon dioxide removal durability, and base cations source uncertainties.

To enable sustainable year-on-year MP1 application, crushed silicate rocks could periodically be introduced in fields with a low content of native silicates. The application of crushed rock (e.g., basalt, olivine, wollastonite) on agricultural soils for CDR (i.e., enhanced rock weathering—ERW) has been demonstrated previously (Holzer et al. 2023; Kantola et al. 2023; Larkin et al. 2022; Xu et al. 2024; Kelland et al. 2020). Co-application of MP1 with crushed rock may accelerate the rate of ERW and improve the overall CDR potential of both approaches, while at the same time providing benefits to soil fertility. The mechanism presented in this paper demonstrates the potential of applying MP1 on farmland to remove carbon dioxide. By applying MP1 across millions of acres, by itself or in combination with crushed silicate rocks, this approach could become an important CDR tool with global impact.

Author Contributions

Tania Timmermann: conceptualization, data curation, formal analysis, funding acquisition, investigation, methodology, project administration, supervision, writing – original draft, writing – review and editing. **Christopher Yip:** formal analysis, investigation, methodology, writing – original draft, writing – review and editing. **Yun-Ya Yang:** formal analysis, investigation, methodology, writing – original draft, writing – review and editing. **Kimberly A. Wemmer:** formal analysis, investigation, methodology, writing – original draft, writing – review and editing. **Anupam Chowdhury:** formal analysis, investigation, writing – original draft. **Daniel Dores:** formal analysis, investigation, methodology, writing – original draft. **Taichi Takayama:** investigation, methodology, software. **Sharon Nademanee:** conceptualization, investigation, methodology, supervision. **Bjorn A. Traag:** supervision, writing – original draft. **Kazem Zamanian:** formal analysis, writing – review and editing. **Bernardo González:** formal analysis, writing – review and editing. **Daniel O. Breecker:** formal analysis, visualization, writing – review and editing. **Noah Fierer:** formal analysis, writing – review and editing. **Eric W. Slessarev:** formal analysis, writing – review and editing. **Gonzalo A. Fuenzalida-Meriz:** conceptualization, data curation, formal analysis, funding acquisition, visualization, writing – review and editing.

Acknowledgments

We thank John L. Grimsich at University of California Berkeley Earth and Planetary Science Department (UCB EPS) for his training, expertise, and facility use on the UCB EPS scanning electron microscope and X-ray diffractometer.

Conflicts of Interest

The authors declare potential competing interests as follows: Tania Timmermann, Christopher Yip, Yun-Ya Yang, Kimberly A. Wemmer, Anupam Chowdhury, Daniel Dores, Taichi Takayama, Sharon Nademanee, Bjorn A. Traag, and Gonzalo Fuenzalida-Meriz are employed by Andes Ag Inc., the company that funded this study. The

authors Kazem Zamanian, Bernardo Gonzalez, Daniel Breecker, and Noah Fierer are compensated members of the scientific advisory board of Andes Ag Inc.

Data Availability Statement

The data that support the findings of this study are openly available in Zenodo at https://doi.org/10.5281/zenodo.15215207.

References

Ahmad, A., N. Chattopadhyay, J. Mandal, N. Mandal, and M. Ghosh. 2020. "Effect of Potassium Solubilizing Bacteria and Waste Mica on Potassium Uptake and Dynamics in Maize Rhizosphere." *Journal of the Indian Society of Soil Science* 68, no. 4: 431–442.

Ahmed, E., and S. J. Holmström. 2014. "Siderophores in Environmental Research: Roles and Applications." *Microbial Biotechnology* 7, no. 3: 196–208. https://doi.org/10.1111/1751-7915.12117.

Ahmed, E., and S. J. Holmström. 2015. "Microbe–Mineral Interactions: The Impact of Surface Attachment on Mineral Weathering and Element Selectivity by Microorganisms." *Chemical Geology* 403: 13–23. https://doi.org/10.1016/j.chemgeo.2015.03.009.

Aloo, B. N., B. A. Makumba, and E. R. Mbega. 2019. "The Potential of Bacilli Rhizobacteria for Sustainable Crop Production and Environmental Sustainability." *Microbiological Research* 219: 26–39.

Amann, T., J. Hartmann, E. Struyf, et al. 2020. "Enhanced Weathering and Related Element Fluxes—A Cropland Mesocosm Approach." *Biogeosciences* 17, no. 1: 103–119. https://doi.org/10.5194/bg-17-103-2020.

American Public Health Association. 1926. *Standard Methods for the Examination of Water and Wastewater*. Vol. 6. American Public Health Association (APHA).

Armstrong McKay, D. I., A. Staal, J. F. Abrams, et al. 2022. "Exceeding 1.5°C Global Warming Could Trigger Multiple Climate Tipping Points." *Science* 377, no. 6611: eabn7950. https://doi.org/10.1126/science.abn7950.

Arnaouteli, S., D. A. Matoz-Fernandez, M. Porter, et al. 2019. "Pulcherrimin Formation Controls Growth Arrest of the *Bacillus subtilis* Biofilm." *Proceedings of the National Academy of Sciences of the United States of America* 116, no. 27: 13553–13562. https://doi.org/10.1073/pnas.190398211631217292.

Azulay, D. N., O. Spaeker, M. Ghrayeb, et al. 2022. "Multiscale X-Ray Study of *Bacillus subtilis* Biofilms Reveals Interlinked Structural Hierarchy and Elemental Heterogeneity." *Proceedings of the National Academy of Sciences of the United States of America* 119, no. 4: e2118107119. https://doi.org/10.1073/pnas.211810711935042817.

Banfield, J. F., W. W. Barker, S. A. Welch, and A. Taunton. 1999. "Biological Impact on Mineral Dissolution: Application of the Lichen Model to Understanding Mineral Weathering in the Rhizosphere." *Proceedings of the National Academy of Sciences of the United States of America* 96, no. 7: 3404–3411.

Barker, W. W., S. A. Welch, and J. F. Banfield. 1997. "Biogeochemical Weathering of Silicate Minerals." *Reviews in Mineralogy* 35: 391–428.

Basak, B. B., and D. R. Biswas. 2009. "Influence of Potassium Solubilizing Microorganism (*Bacillus mucilaginosus*) and Waste Mica on Potassium Uptake Dynamics by Sudan Grass (*Sorghum vulgare* Pers.) Grown Under Two Alfisols." *Plant and Soil* 317: 235–255.

Beerling, D. J., D. Z. Epihov, I. B. Kantola, et al. 2024. "Enhanced Weathering in the US Corn Belt Delivers Carbon Removal With Agronomic Benefits." *Proceedings of the National Academy of Sciences of the United States of America* 121, no. 9: e2319436121. https://doi.org/10.1073/pnas.2319436121386712.

Boquet, E., A. Boronat, and A. Ramos-Cormenzana. 1973. "Production of Calcite (Calcium Carbonate) Crystals by Soil Bacteria Is a General Phenomenon." *Nature* 246, no. 5434: 527–529.

Bramble, D. S. E., S. Ulrich, I. Schöning, et al. 2024. "Formation of Mineral-Associated Organic Matter in Temperate Soils Is Primarily Controlled by Mineral Type and Modified by Land Use and Management Intensity." *Global Change Biology* 30, no. 1: e17024. https://doi.org/10.1111/gcb.17024.

Brantley, S. L., A. Shaughnessy, M. I. Lebedeva, and V. N. Balashov. 2023. "How Temperature-Dependent Silicate Weathering Acts as Earth's Geological Thermostat." *Science* 379, no. 6630: 382–389.

Chadwick, O. A., J. Chorover, K. D. Chadwick, et al. 2022. "Constraints of Climate and Age on Soil Development in Hawai'i." In *Biogeochemistry of the Critical Zone*, 49–88. Springer International Publishing.

Combs, S. M., and M. V. Nathan. 1998. "Soil Organic Matter." In *Recommended Chemical Soil Test Procedures for the North Central Region*, edited by J. R. Brown, vol. 221, 53–58. Missouri Agriculture Experiment Station.

Connerty, H. V., and A. R. Briggs. 1966. "Determination of Serum Calcium by Means of Orthocresolphthalein Complexone." *American Journal of Clinical Pathology* 45, no. 3: 290–296. https://doi.org/10.1093/ajcp/45.3.290.

EPA, U.S. 1996. *Method 3050B: Acid Digestion of Sediments, Sludges, and Soils*. Environmental Protection Agency.

Ercole, C., P. Bozzelli, F. Altieri, P. Cacchio, and M. Del Gallo. 2012. "Calcium Carbonate Mineralization: Involvement of Extracellular Polymeric Materials Isolated From Calcifying Bacteria." *Microscopy and Microanalysis* 18, no. 4: 829–839.

Fierer, N., and C. M. Walsh. 2023. "Can We Manipulate the Soil Microbiome to Promote Carbon Sequestration in Croplands?" *PLoS Biology* 21, no. 7: e3002207.

Finlay, R. D., S. Mahmood, N. Rosenstock, et al. 2020. "Reviews and Syntheses: Biological Weathering and Its Consequences at Different Spatial Levels–From Nanoscale to Global Scale." *Biogeosciences* 17, no. 6: 1507–1533. https://doi.org/10.5194/bg-17-1507-2020.

Frey, B., S. R. Rieder, I. Brunner, et al. 2010. "Weathering-Associated Bacteria From the Damma Glacier Forefield: Physiological Capabilities and Impact on Granite Dissolution." *Applied and Environmental Microbiology* 76, no. 14: 4788–4796. https://doi.org/10.1128/AEM.00657-10.

Gruber, C., C. Zhu, R. B. Georg, Y. Zakon, and J. Ganor. 2014. "Resolving the Gap Between Laboratory and Field Rates of Feldspar Weathering." *Geochimica et Cosmochimica Acta* 147: 90–106.

Han, M., X. Zhu, C. Ruan, et al. 2024. "Micro-Biophysical Interactions at Bacterium-Mineral Interfaces Determine Potassium Dissolution." *Environmental Technology & Innovation* 33: 103524. https://doi.org/10.1016/j.eti.2023.103524.

Han, Z., X. Gao, H. Zhao, et al. 2018. "Extracellular and Intracellular Biomineralization Induced by *Bacillus licheniformis* DB1-9 at Different Mg/Ca Molar Ratios." *Minerals* 8, no. 12: 585. https://doi.org/10.3390/min8120585.

Han, Z., J. Wang, H. Zhao, et al. 2019. "Mechanism of Biomineralization Induced by *Bacillus subtilis* J2 and Characteristics of the Biominerals." *Minerals* 9, no. 4: 218. https://doi.org/10.3390/min9040218.

Hartmann, J., and N. Moosdorf. 2012. "The New Global Lithological Map Database GLiM: A Representation of Rock Properties at the Earth Surface." *Geochemistry, Geophysics, Geosystems* 13, no. 12: 1–37. https://doi.org/10.1029/2012GC004370.

Holzer, I. O., M. A. Nocco, and B. Z. Houlton. 2023. "Direct Evidence for Atmospheric Carbon Dioxide Removal via Enhanced Weathering

in Cropland Soil." *Environmental Research Communications* 5, no. 10: 101004.

Homann, M., P. Sansjofre, M. Van Zuilen, et al. 2018. "Microbial Life and Biogeochemical Cycling on Land 3,220 Million Years Ago." *Nature Geoscience* 11, no. 9: 665–671. https://doi.org/10.1038/s41561-018-0190-9.

Kalamara, M., J. C. Abbott, C. E. MacPhee, and N. R. Stanley-Wall. 2021. "Biofilm Hydrophobicity in Environmental Isolates of *Bacillus subtilis*." *Microbiology* 167, no. 9: 001082. https://doi.org/10.1099/mic.0.001082.

Kantola, I. B., E. Blanc-Betes, M. D. Masters, et al. 2023. "Improved Net Carbon Budgets in the US Midwest Through Direct Measured Impacts of Enhanced Weathering." *Global Change Biology* 29, no. 24: 7012–7028. https://doi.org/10.1111/gcb.16903.

Kelland, M. E., P. W. Wade, A. L. Lewis, et al. 2020. "Increased Yield and CO_2 Sequestration Potential With the C4 Cereal *Sorghum bicolor* Cultivated in Basaltic Rock Dust-Amended Agricultural Soil." *Global Change Biology* 26, no. 6: 3658–3676. https://doi.org/10.1111/gcb.15089.

Kemmling, A., M. Kämper, C. Flies, O. Schieweck, and M. Hoppert. 2004. "Biofilms and Extracellular Matrices on Geomaterials." *Environmental Geology* 46, no. 3: 429–435.

Kim, H. J., B. Shin, Y. S. Lee, and W. Park. 2017. "Modulation of Calcium Carbonate Precipitation by Exopolysaccharide in *Bacillus* sp. JH7." *Applied Microbiology and Biotechnology* 101: 6551–6561.

Kraemer, S. M. 2004. "Iron Oxide Dissolution and Solubility in the Presence of Siderophores." *Aquatic Sciences* 66: 3–18.

Lal, R., and J. M. Kimble. 2000. "Pedogenic Carbonates and the Global Carbon Cycle." In *Global Climate Change and Pedogenic Carbonates*, edited by R. Lal, J. M. Kimble, H. Eswaran, and B. A. Stewart. CRC Press.

Larkin, C. S., M. G. Andrews, C. R. Pearce, et al. 2022. "Quantification of CO_2 Removal in a Large-Scale Enhanced Weathering Field Trial on an Oil Palm Plantation in Sabah, Malaysia." *Frontiers in Climate* 4: 959229. https://doi.org/10.3389/fclim.2022.959229.

Lee, J. H., J. K. Fredrickson, R. K. Kukkadapu, et al. 2012. "Microbial Reductive Transformation of Phyllosilicate Fe (III) and U (VI) in Fluvial Subsurface Sediments." *Environmental Science & Technology* 46, no. 7: 3721–3730. https://doi.org/10.1021/es204528m.

Lian, B., Q. Hu, J. Chen, J. Ji, and H. H. Teng. 2006. "Carbonate Biomineralization Induced by Soil Bacterium *Bacillus megaterium*." *Geochimica et Cosmochimica Acta* 70, no. 22: 5522–5535.

Liu, W., X. Xu, X. Wu, Q. Yang, Y. Luo, and P. Christie. 2006. "Decomposition of Silicate Minerals by *Bacillus mucilaginosus* in Liquid Culture." *Environmental Geochemistry and Health* 28: 133–140.

Marçais, G., A. L. Delcher, A. M. Phillippy, R. Coston, S. L. Salzberg, and A. Zimin. 2018. "MUMmer4: A Fast and Versatile Genome Alignment System." *PLoS Computational Biology* 14, no. 1: e1005944.

Marschner, H., ed. 2011. *Marschner's Mineral Nutrition of Higher Plants*. Academic Press.

McConnaughey, T. A., and J. F. Whelan. 1997. "Calcification Generates Protons for Nutrient and Bicarbonate Uptake." *Earth-Science Reviews* 42, no. 1–2: 95–117.

Mo, B., and B. Lian. 2011. "Interactions Between *Bacillus Mucilaginosus* and Silicate Minerals (Weathered Adamellite and Feldspar): Weathering Rate, Products, and Reaction Mechanisms." *Chinese Journal of Geochemistry* 30: 187–192.

Moorehead, W. R., and H. G. Biggs. 1974. "2-Amino-2-Methyl-1-Propanol as the Alkalizing Agent in an Improved Continuous-Flow Cresolphthalein Complexone Procedure for Calcium in Serum." *Clinical Chemistry* 20, no. 11: 1458–1460.

Nelson, D. W., and L. E. Sommers. 1996. "Total Carbon, Organic Carbon, and Organic Matter." In *Methods of Soil Analysis: Part 3 Chemical Methods*, edited by D. L. Sparks, A. L. Page, P. A. Helmke, et al., vol. 5, 961–1010. American Society of Agronomy, Crop Science Society of America, and Soil Science Society of America.

Newman, D. K., and R. Kolter. 2000. "A Role for Excreted Quinones in Extracellular Electron Transfer." *Nature* 405, no. 6782: 94–97.

Niron, H., A. Vienne, P. Frings, R. Poetra, and S. Vicca. 2024. "Exploring the Synergy of Enhanced Weathering and *Bacillus subtilis*: A Promising Strategy for Sustainable Agriculture." *Global Change Biology* 30, no. 9: e17511.

Nishikawa, M., and K. Kobayashi. 2021. "Calcium Prevents Biofilm Dispersion in *Bacillus subtilis*." *Journal of Bacteriology* 203, no. 14: 10–1128.

NOAA National Centers for Environmental Information (NCEI). 2024. *Climate Data Online (CDO)*. U.S. National Oceanic and Atmospheric Administration. https://www.ncei.noaa.gov/cdo-web/.

Okrusch, M., and H. E. Frimmel. 2020. *Mineralogy: An Introduction to Minerals, Rocks, and Mineral Deposits*. Springer Nature.

Paidhungat, M., B. Setlow, A. Driks, and P. Setlow. 2000. "Characterization of Spores of *Bacillus subtilis* Which Lack Dipicolinic Acid." *Journal of Bacteriology* 182, no. 19: 5505–5512.

Peters, J. B., M. V. Nathan, C. A. M. Laboski, and M. Nathan. 2012. "pH and Lime Requirement. Ch. 4." In *Recommended Chemical Soil Test Procedures for the North Central Region*, vol. 221, 16–22. University of Missouri.

Potapov, P., S. Turubanova, M. C. Hansen, et al. 2022. "Global Maps of Cropland Extent and Change Show Accelerated Cropland Expansion in the Twenty-First Century." *Nature Food* 3, no. 1: 19–28. https://doi.org/10.1038/s43016-021-00429-z.

Power, I. M., V. N. Hatten, M. Guo, Z. R. Schaffer, K. Rausis, and H. Klyn-Hesselink. 2025. "Are Enhanced Rock Weathering Rates Overestimated? A Few Geochemical and Mineralogical Pitfalls." *Frontiers in Climate* 6: 1510747. https://doi.org/10.3389/fclim.2024.1510747.

Quast, C., E. Pruesse, P. Yilmaz, et al. 2012. "The SILVA Ribosomal RNA Gene Database Project: Improved Data Processing and Web-Based Tools." *Nucleic Acids Research* 41, no. D1: D590–D596. https://doi.org/10.1093/nar/gks1219.

Reershemius, T., M. E. Kelland, J. S. Jordan, et al. 2023. "Initial Validation of a Soil-Based Mass-Balance Approach for Empirical Monitoring of Enhanced Rock Weathering Rates." *Environmental Science & Technology* 57, no. 48: 19497–19507. https://doi.org/10.1021/acs.est.3c03609.

Ribeiro, I. D. A., C. G. Volpiano, L. K. Vargas, C. E. Granada, B. B. Lisboa, and L. M. P. Passaglia. 2020. "Use of Mineral Weathering Bacteria to Enhance Nutrient Availability in Crops: A Review." *Frontiers in Plant Science* 11: 590774.

Richards, L. A., ed. 1954. *Diagnosis and Improvement of Saline and Alkali Soils (No. 60)*. US Government Printing Office.

Rowley, M. C., S. Grand, and É. P. Verrecchia. 2018. "Calcium-Mediated Stabilisation of Soil Organic Carbon." *Biogeochemistry* 137, no. 1: 27–49. https://doi.org/10.1007/s10533-017-0410-1.

Sanderman, J. 2012. "Can Management Induced Changes in the Carbonate System Drive Soil Carbon Sequestration? A Review With Particular Focus on Australia." *Agriculture, Ecosystems & Environment* 155: 70–77.

Schwengers, O., L. Jelonek, M. A. Dieckmann, S. Beyvers, J. Blom, and A. Goesmann. 2021. "Bakta: Rapid and Standardized Annotation of Bacterial Genomes via Alignment-Free Sequence Identification." *Microbial Genomics* 7, no. 11: 000685. https://doi.org/10.1099/mgen.0.000685.

Sezonov, G., D. Joseleau-Petit, and R. d'Ari. 2007. "*Escherichia Coli* Physiology in Luria-Bertani Broth." *Journal of Bacteriology* 189, no. 23: 8746–8749. https://doi.org/10.1128/JB.01368-07.

Shabtai, I. A., R. C. Wilhelm, S. A. Schweizer, C. Höschen, D. H. Buckley, and J. Lehmann. 2023. "Calcium Promotes Persistent Soil Organic Matter by Altering Microbial Transformation of Plant Litter." *Nature Communications* 14, no. 1: 6609.

Sheng, X. F., F. Zhao, L. Y. He, G. Qiu, and L. Chen. 2008. "Isolation and Characterization of Silicate Mineral-Solubilizing *Bacillus globisporus* Q12 From the Surfaces of Weathered Feldspar." *Canadian Journal of Microbiology* 54, no. 12: 1064–1068.

Sherrod, L. A., G. Dunn, G. A. Peterson, and R. L. Kolberg. 2002. "Inorganic Carbon Analysis by Modified Pressure-Calcimeter Method." *Soil Science Society of America Journal* 66, no. 1: 299–305. https://doi.org/10.2136/sssaj2002.0299.

Smith, D. B., F. Solano, L. G. Woodruff, W. F. Cannon, and K. J. Ellefsen. 2019. *Geochemical and Mineralogical Maps, With Interpretation, for Soils of the Conterminous United States*. U.S. Geological Survey Scientific Investigations Report 2017–5118.

Solomon, S., ed. 2007. *Climate Change 2007—The Physical Science Basis: Working Group I Contribution to the Fourth Assessment Report of the IPCC*. Vol. 4. Cambridge University Press.

Suarez, D. L. 2000. "Impact of Agriculture on CO_2 as Affected by Changes in Inorganic Carbon." In *Global Climate Change and Pedogenic Carbonates*, edited by R. Lal, J. M. Kimble, H. Eswaran, and B. A. Stewart, 257–272. CRC Press.

Sumner, M. E., and W. P. Miller. 1996. "Cation Exchange Capacity and Exchange Coefficients." In *Methods of Soil Analysis: Part 3 Chemical Methods*, edited by D. L. Sparks, A. L. Page, P. A. Helmke, et al., vol. 5, 1201–1229. American Society of Agronomy, Crop Science Society of America, and Soil Science Society of America.

te Pas, E. E., M. Hagens, and R. N. Comans. 2023. "Assessment of the Enhanced Weathering Potential of Different Silicate Minerals to Improve Soil Quality and Sequester CO_2." *Frontiers in Climate* 4: 954064. https://doi.org/10.3389/fclim.2022.954064.

USDA NRCS (U.S. Department of Agriculture Natural Resources Conservation Service). 2024. "Soil Survey Geographic (SSURGO) Database." https://websoilsurvey.sc.egov.usda.gov/App/HomePage.htm.

Vicca, S., D. S. Goll, M. Hagens, et al. 2022. "Is the Climate Change Mitigation Effect of Enhanced Silicate Weathering Governed by Biological Processes?" *Global Change Biology* 28, no. 3: 711–726. https://doi.org/10.1111/gcb.15993.

Vienne, A., S. Poblador, M. Portillo-Estrada, et al. 2022. "Enhanced Weathering Using Basalt Rock Powder: Carbon Sequestration, Co-Benefits and Risks in a Mesocosm Study With *Solanum tuberosum*." *Frontiers in Climate* 4: 869456. https://doi.org/10.3389/fclim.2022.869456.

Walker, J. C., P. B. Hays, and J. F. Kasting. 1981. "A Negative Feedback Mechanism for the Long-Term Stabilization of Earth's Surface Temperature." *Journal of Geophysical Research: Oceans* 86, no. C10: 9776–9782. https://doi.org/10.1029/JC086iC10p09776.

Warnacke, D., and J. R. Brown. 2015. "Potassium and Other Basic Cations." In *Recommended Chemical Soil Testing Procedures for the North Central Region*. North Central Regional Research Publication No. 221 (revised), edited by M. V. Nathan and R. H. Gelderman, 7.1–7.3. Missouri Agricultural Experiment Station SB 1001.

White, A. F., and S. L. Brantley. 2003. "The Effect of Time on the Weathering of Silicate Minerals: Why Do Weathering Rates Differ in the Laboratory and Field?" *Chemical Geology* 202, no. 3–4: 479–506.

Whitney, D. A. 2015. "Micronutrients: Zinc, Iron, Manganese and Copper." In *Recommended Chemical Soil Testing Procedures for the North Central Region*. North Central Regional Research Publication No. 221 (revised), edited by M. V. Nathan and R. H. Gelderman, 9.1–9.4. Missouri Agricultural Experiment Station SB 1001.

Wild, B., R. Gerrits, and S. Bonneville. 2022. "The Contribution of Living Organisms to Rock Weathering in the Critical Zone." *Npj Materials Degradation* 6, no. 1: 98.

Wild, B., G. Imfeld, and D. Daval. 2021. "Direct Measurement of Fungal Contribution to Silicate Weathering Rates in Soil." *Geology* 49, no. 9: 1055–1058.

Wilson, M. J. 2004. "Weathering of the Primary Rock-Forming Minerals: Processes, Products and Rates." *Clay Minerals* 39, no. 3: 233–266.

Xavier, G. R., E. D. C. Jesus, A. Dias, M. R. R. Coelho, Y. C. Molina, and N. G. Rumjanek. 2023. "Contribution of Biofertilizers to Pulse Crops: From Single-Strain Inoculants to New Technologies Based on Microbiomes Strategies." *Plants* 12, no. 4: 954. https://doi.org/10.3390/plants12040954.

Xiao, L., B. Lian, J. Hao, C. Liu, and S. Wang. 2015. "Effect of Carbonic Anhydrase on Silicate Weathering and Carbonate Formation at Present Day CO_2 Concentrations Compared to Primordial Values." *Scientific Reports* 5, no. 1: 7733.

Xu, T., Z. Yuan, S. Vicca, et al. 2024. "Enhanced Silicate Weathering Accelerates Forest Carbon Sequestration by Stimulating the Soil Mineral Carbon Pump." *Global Change Biology* 30, no. 8: e17464. https://doi.org/10.1111/gcb.17464.

Yip, C., P. D. Weyman, K. A. Wemmer, et al. 2025. "Quantification of Soil Inorganic Carbon Using Sulfamic Acid and Gas Chromatography." *PLoS One*.

Zamanian, K., and Y. Kuzyakov. 2022. "Soil Inorganic Carbon: Stocks, Functions, Losses and Their Consequences." In *Burleigh Dodds Series in Agricultural Science*, 209–236. EGU General Assembly.

Zhao, M., Y. Zhao, W. Lin, and K. Q. Xiao. 2023. "An Overview of Experimental Simulations of Microbial Activity in Early Earth." *Frontiers in Microbiology* 13: 1052831.

Zhuang, D., H. Yan, M. E. Tucker, et al. 2018. "Calcite Precipitation Induced by *Bacillus cereus* MRR2 Cultured at Different Ca^{2+} Concentrations: Further Insights Into Biotic and Abiotic Calcite." *Chemical Geology* 500: 64–87. https://doi.org/10.1016/j.chemgeo.2018.09.018.

Supporting Information

Additional supporting information can be found online in the Supporting Information section.